Catalysis Science & Technology

Accepted Manuscript

ROYAL SOCIETY OF CHEMISTRY

rsc.li/catalysis

View Article Online
DOI: 10.1039/C8CY01448E

Catalysis Science & Technology

ARTICLE

Engineering P450$_{LaMO}$ Stereospecificity and Product Selectivity for Selective C-H Oxidation of Tetralin-like Alkylbenzenes

Received 00th January 20xx,
Accepted 00th January 20xx

DOI: 10.1039/x0xx00000x

www.rsc.org/

Ren-Jie Li,[a] Aitao Li,[b] Jing Zhao,[c] Qi Chen,[a] Ning Li,[d] Hui-Lei Yu[a]* and Jian-He Xu[a]

P450-mediated asymmetric hydroxylation of inert C-H bond is a chemically challenging reaction. Self-sufficient P450$_{LaMO}$ from CYP116B subfamily could catalyze the transformation of 1,2,3,4-tetrahydronaphthalene to (*S*)-tetralol, despite with poor enantioselectivity (*er* 66:34) and product selectivity (the ratio of alcohol and ketone, *ak*, 76:24). To improve the selectivity, phenyalanine scanning and further protein engineering were performed to reshape the active pocket of P450$_{LaMO}$, resulting in a mutant (T121V/Y385F/M391L) with not only improved (*S*)-enantioselectivity (*er* 98:2) but also excellent product selectivity (*ak* 99:1), in contrast to another mutant L97F/T121F/E282V/T283Y with complementary (*R*)-enantioselectivity (*er* 23:77). Moverover, the enantiopure (*S*)-alcohols formed by P450$_{LaMO}$-catalyzed oxidation for a series of alkylbenzenes are potentially important building blocks in the pharmaceutical industry. This Phe-based enantioselectivity engineering used for reshaping the active pocket of P450s could provide a guide to the protein evolution of other CYP116B members.

Introduction

Biocatalysis plays an important role in green and sustainable synthesis of enantiopure compounds, especially chiral alcohols.[1] The asymmetric hydroxylation of inert C-H bonds could be achieved by traditional chemical methods, but they are generally costly, energy-intensive and non-selective.[2] The P450 (Cytochrome P450)-mediated asymmetric hydroxylation of inert C-H bond is of great interest and has a great potential to form highly enantiopure hydroxylated products.[3]

P450s catalyze various chemically challenging reactions, such as non-activated C-H hydroxylation, alkene epoxidation and sulfoxidation.[4] The typical representatives (*e.g.* P450$_{cam}$,[5] P450$_{pyr}$[6] and P450$_{BM3}$[7]) displayed high activity and excellent regio-/enantioselectivity after being tailored by molecular engineering approaches. For example, the evolved P450$_{BM3}$ variants show impressive promiscuous activity[8] and can be used for obtaining the products of carbene[9] and nitrene transfer[10] with high enantioselectivity. Another self-sufficient CYP116B member, P450$_{LaMO}$,[11] belonging to Class VII monooxygenase, contains novel FMN and Fe_2S_2 domains for conducting electrons transfer to the heme domain.[12] This type of P450 monooxygenases are reported to be able to perform C-H hydroxylation,[13] *O*-demethylation,[14] styrene epoxidation[5] and sulfide oxidation.[15] Recently, it was reported that P450$_{LaMO}$ could be used for *anti*-Markovnikov addition of styrene derivatives, with an improved activity and selectivity after directed evolution.[11]

It is known that (*S*)-tetralol can be used as a key intermediate for synthesis of bioactive compounds, such as prodrugs of meropenem, JAK3 inhibitor and ORL-1 receptor agonist.[16] Whereas very few reports are available regarding P450 monooxygenase catalyzed production of (*S*)-tetralol,[17] several of the self-sufficient CYP116B members, including P450$_{RpMO}$, P450$_{CtMO}$ and P450$_{ArMO}$, were employed for asymmetric oxidation of the core structure of tetralin (**1a**) into tetralol (**2a**).[14b] Particularly, the native P450$_{LaMO}$ was able to convert 1a into (*S*)-**2a** despite of the poor enantioselectivity (*er* 66:34, *S*/*R*) and product selectivity (alcohol : ketone, *ak* 76:24). Therefore, this research was focused on the directed evolution of P450$_{LaMO}$ for producing (*S*)-tetralol and other chiral alcohols (Scheme 1) with better product selectivity and enantioselectivity.

[a] State Key Laboratory of Bioreactor Engineering, Shanghai Collaborative Innovation Center for Biomanufacturing, East China University of Science and Technology, 130 Meilong Road, Shanghai 200237, P. R. China. E-mail: huileiyu@ecust.edu.cn
[b] Hubei Collaborative Innovation Center for Green Transformation of Bio-resources, Hubei Key Laboratory of Industrial Biotechnology, College of Life Sciences, Hubei University, Wuhan 430062, P. R. China.
[c] Tianjin Institute of Industrial Biotechnology, Chinese Academy of Sciences, Tianjin 300308, P. R. China.
[d] State Key Laboratory of Pulp and Paper Engineering, College of Light Industry and Food Sciences, South China University of Technology, Guangzhou, 510640, China.
†Electronic Supplementary Information (ESI) available: Additional data, chromatograms, MS and NMR data. See DOI: 10.1039/x0xx00000x

View Article Online
DOI: 10.1039/C8CY01448E

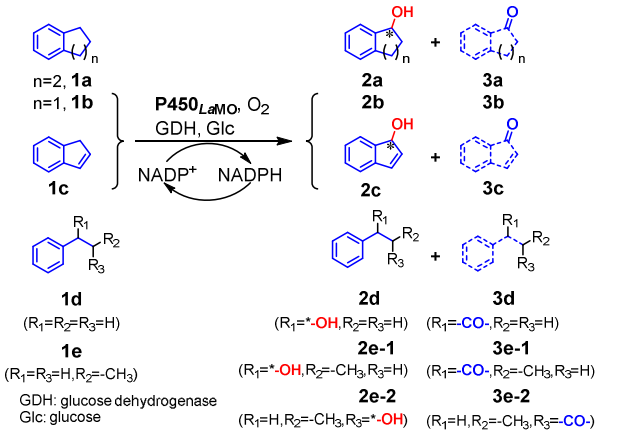

Scheme 1 Cytochrome P450$_{LaMO}$ catalysed asymmetric hydroxylation of alkylbenzenes to form corresponding (*S*)-alcohols.

Thus far, various approaches have been proffered on reshaping the active pocket of enzymes[18] to improve the enantioselectivity, such as single codon saturation mutagenesis (SCSM), double codon saturation mutagenesis (DCSM) and triple codon saturation mutagenesis (TCSM).[18i,19] However, there was no systematical study on probing the active pocket of P450$_{LaMO}$ to enhance its enantioselectivity. Herein, we tried to improve the stereoselectivity and product selectivity through phenylalanine (Phe)-based scanning to reshape the active pocket, followed by polarity optimization of active pocket with valine.

Experimental

Materials

1,2,3,4-Tetrahydronaphthalene and alkylbenzenes compounds and the corresponding racemic alcohol standards used in this work were of analytical grade and commercially available. *δ*-Aminolevulinic acid hydrochloride, isopropyl *β*-D-1-thiogalactopyranoside (IPTG, >99%) and kanamycin disulfate salt (>99%) was from Sangon (Shanghai, China). PrimeSTAR HS DNA polymerase was obtained from TaKaRa (Shanghai, China). *Dpn*I was purchased from New England Biolabs (Beverley, MA). Plasmid pRSFDuet1 was obtained from Novagen (Madison, WI). Tryptone and yeast extract were purchased from OXOID (Shanghai, China), NaCl, K_2HPO_4, KH_2PO_4 were commercially available. *Escherichia coli* competent cells BL21 (DE3) were prepared using a standard protocol.[20] Sequence analysis was performed by Sain biological (Shanghai, China).

High throughput screening process for enantioselectivity evolution

Single colonies were picked with toothpicks, inoculated and grown at 37 °C in 96-deep well plates with 300 µL LB medium per well, containing 50 mg/L kanamycin, using wildtype as the positive control. The expression culture was inoculated by transferring 50 µL overnight culture into 650 µL Terrific Broth medium supplemented with 50 mg/L kanamycin. When the OD_{600} reached ~1.0, 0.2 mM IPTG (isopropyl-*β*-D-thiogalactopyranoside) and 0.2 mM ALA (5-aminolevulinic acid hydrochloride) were added to each well and the temperature was decreased to 16 °C for incubation for another 24 h. The cells were then harvested by centrifugation (3220 × *g*, 10 min). The cell pellets were resuspended in 300 µL potassium phosphate buffer (100 mM, pH 8.0, saturated with oxygen) and transferred into 96-well microplates.

The reaction mixture (150 µL), containing whole cells expressing P450$_{LaMO}$ (1.6 g CDW/L), 1.0 mM 1,2,3,4-tetrahydronaphthalene, and 100 mM KPi buffer (pH 8.0) in 96-deep well plates, was incubated at 220 rpm for 5 h. Then, the mixture was separated by centrifuge (3220 × *g*, 15 min) and 130 µL supernatant was dispensed into two new microplates to perform further dehydrogenation. The dehydrogenation was started by separately adding 10 µL *Cp*CR (0.5 U) and 10 µL mixed NBT-PMS solution (NBT 2 mg/mL, PMS 0.1 mg/mL and $NADP^+$ 0.3 mM), and then the change in absorbance at 580 nm was monitored after the reaction was kept at 30 °C for 1 h in the dark (Fig. S1† and Table S5†).

Measurement of Total Turnover Number and Turnover frequency

All of the enzymatic transformations were performed in 1-mL reaction tubes on a mini-shaker (HLCBioTech, MHR23) at 600 rpm, 20 °C, 5 min. The reaction mixtures (1 mL) were composed of 0.2 µM P450s,[21] 0.5 mM NADPH and 0.5 mM substrate. The total turnover number (TTN) of reactions were measured at 1-mL scale in 5 mL crimp vials using oxygen saturated KPi buffer (100 mM, pH 8.0) containing 0.8 µM purified P450, 5 mM substrate, 0.5 mM $NADP^+$, 15 U/mL glucose dehydrogenase, and 20 mM glucose. The vials were sealed and stirred for 12 h at 25 °C and 180 rpm. Then 500 µL ethyl acetate was used (with 0.5 mM guaiacol as an internal standard) to extract the sample twice, and the organic layers were combined and dried over anhydrous Na_2SO_4. Subsequently, the extract was concentrated to 50 µL to perform GC-MS analysis for quantitation of the reaction product. For more details, see the ESI.

Molecular Docking and Mutation Site Exhibition

A structural model of P450$_{LaMO}$ wildtype was constructed based on the crystal structures of its homologue enzyme P450TT (CYP116B46) (PDB ID: 6GII, 1.9 Å, 55% identity to P450$_{LaMO}$). The online SWISS-MODEL web server (http://www.swissmodel. expasy.org/) was used to perform the homology modeling (the assessment of the homologous modelling was shown in Fig S8, ESI).[22] The 3D structure of substrate tetralin was generated by energy minimization. Then the substrate structure was docked into the binding pocket of the constructed P450$_{LaMO}$ model (AutoDock 4.0). The best scoring results were selected for structural comparison and catalytic mechanism analysis. After introducing mutagenesis, the mutation sites were shown by the visual software Pymol 2.5.

Preparative Hydroxylation Reaction

The preparative hydroxylation reactions were performed according to the earlier stated procedure: The 125-mL scale

View Article Online
DOI: 10.1039/C8CY01448E

reaction was performed in a 500-mL grinding mouth reactor, containing 2 μM P450 (purified enzymes),[21] 20 mM glucose, 4 mM substrate, 15 U glucose dehydrogenase, and 0.5 mM $NADP^+$ in KPi buffer (100 mM, pH 8.0). The reaction was carried out at 25 °C with magnetic stirring for 12 h. After completion, the reaction mixture was extracted with ethyl acetate (100 mL × 2) and the organic phase was dried, concentrated and subjected to gas chromatography to analyze the product formation.

Analytical instruments and methods

Analytical high-performance liquid chromatography (HPLC) was performed with Shimadzu 2010A Infinity instrument using an OD-H column (Daicel, 4.6 × 5 mm, 2.7 μm) with *n*-hexane and isopropanol as the mobile phase to analyze the enantioselectivity. All measurements were performed with a Shimadzu 2010 Infinity Diode Array Detector and the recorded wavelength was set at 254 nm.

Gas chromatography (GC) analyses were carried out with a Shimadzu GC-2014 instrument equipped with a flame ionization detector using an Agilent Rsi-MS column (30 m × 0.32 mm, 0.25 μm film) with nitrogen as carrier gas to analyze the product distribution. Injector temperature: 280 °C. Split mode with a split ratio of 10. Detector temperature: 280 °C.

Chiral GC analysis was conducted with an Agilent 7820A instrument equipped with a flame ionization detector using a chiral Agilent CP column (30 m × 0.32 mm, 0.25 μm film) with helium as carrier gas to analyze the configuration of products. Injector temperature: 200 °C. Split mode with a split ratio of 5. Detector temperature: 280 °C. The retention time of all the compounds see the ESI.[11a]

NMR data

Two products **2a** and **2d** were selected to perform the NMR analysis. Another four products' configuration confirmed by the previous work,[11a] NMR spectra see ESI. More details are as follows:

Data for **2a**, (*S*)-1,2,3,4-tetrahydronaphthalen-1-ol. ^{1}H NMR (400 MHz, DMSO-d_6) δ 7.37-7.33 (m, 1H), 7.13-7.08 (m, 2H), 7.03-7.01 (m, 1H), 5.05-5.03 (br, 1H), 4.56-4.52 (m, 1H), 2.76-2.60 (m, 2H), 1.88-1.64 (m, 4H). ^{13}C NMR (100 MHz, DMSO-d_6) δ 145.5, 141.6, 133.6, 133.5, 131.8, 130.7, 71.6, 37.5, 34.0, 24.3.

Data for **2d**, (*S*)-1-phenylenthan-1-ol. ^{1}H NMR (400 MHz, $CDCl_3$): δ = 7.37-7.27 (m, 5H), 4.88 (q, *J* = 4.0 Hz, 1H), 2.06 (s, 1H), 1.48 (d, *J* = 4.0 Hz, 3H).^{13}C NMR (100 MHz, $CDCl_3$): δ 145.8, 128.6, 127.5, 125.4, 70.4, 25.2.

Results and discussion

To enhance the enantioselectivity, the Phe-substituting mutagenesis at five selected residues (L97, T121, V123, N124 and A275) lining the active pocket of $P450_{LaMO}$ was firstly performed (Fig. 1A).[18i,19f] Instead of mutating these sites by the single site saturation mutagenesis (with NNK codon degeneracy), Phe scan was employed based on its non-polarity, larger hindrance and hydrophobic side chain properties, which is considered to be more liable for reshaping the active pocket. Among the resultant 5 mutants, RJ1 (T121F) showed improved (*S*)-enantioselectivity (*er* 93:7). Interestingly, another mutant RJ4 (L97F) inverted the enantioselectivity, forming (*R*)-product with an *er* of 47:53 (*Step 1* in Scheme 2). The mutation at the remaining three sites did not affect the enantioselectivity, giving similar *er* values with that of the wildtype. Subsequently, two rounds of NNK-based saturation mutagenesis were performed at other four (Y385, M391, M326, V327, Fig. 1B) sites surrounding the heme, based on iterative saturation mutagenesis (ISM) of variant RJ1 (*Step 2* in Scheme 2). The selectivity screening was conducted by a colorimetric assay of dehydrogenase coupled with NBT-PMS (Fig. S1† and Table S5†). The resulting mutant RJ2 (T121F/Y385F/M391L) further improved the *er* to 95:5 and *ak* to 95:5, enhancing the TOF and TTN by 4.3-fold and 7.1-fold over WT, respectively. In order to further enhance the selectivity, we optimized the polarity and hindrance by single-site mutagenesis (SSM) on residue T121 of RJ2, resulting in mutant RJ3 (T121V/Y385F/M329L, *Step 3* in Scheme 2). It gave the highest enantioselectivity with an *er* of up to 98:2 (*S*/*R*), and almost no side product was detected (*ak* 99:1, Fig. S3† and Fig. S4†). Furthermore, we found that mutant RJ33 (T121P/Y385F/M329L, Table S4†) displayed higher activity after polarity optimization on site T121 in the active pocket in spite of a slightly decreased *er* (94:6).

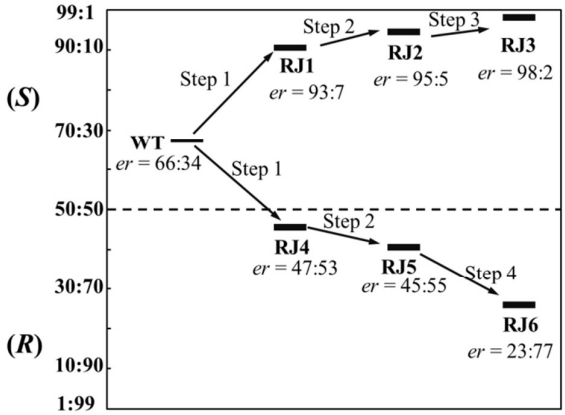

Scheme 2 Directed evolution pathways producing the (*S*)- or (*R*)-selective $P450_{LaMO}$ mutants as catalysts for the asymmetric hydroxylation of substrate **1a**. Step 1: phenylalanine scan. Step 2: iterative saturation mutagenesis. Step 3: single site saturation mutagenesis. Step 4: combinatorial mutagenesis.

In Step 1, RJ4 (L97F) inverted the enantioselectivity. To further improve the (*R*)-enantioselectivity, double site semi-saturation mutagenesis (with NDT codon degeneracy) was carried out based on RJ4 (L97F).[18a,23] About 1600 randomization variants (with 95% coverage) focusing on sites L97-K99, H206-W211, E282-T283 and A279-A280 (internal and outside active pocket, Fig. 1B) were screened.[24] However, the (*R*)-selectivity was not obviously enhanced and the resulting mutant RJ5 (L97F/E282V/T283Y) yielded the (*R*)-alcohol with *er* 45:55 and *ak* 91:9 (*Step 2* in Scheme 2, Table S6†). Moreover, the catalytic efficiency was promoted, with increases of TOF and TTN by 1.8-fold and 2.4-fold, respectively. When

View Article Online
DOI: 10.1039/C8CY01448E

introducing the mutation of T121F into variant RJ5, the resulting variant RJ6 (L97F/T121F/E282V/T283Y, *Step 4* in Scheme 2) improved the (*R*)-selectivity from *er* 45:55 (*S*/*R*) to *er* 23:77, although the activity (TOF: 0.02 min^{-1}) was reduced by half compared to wildtype (TOF: 0.04 min^{-1}) (Table S6†).

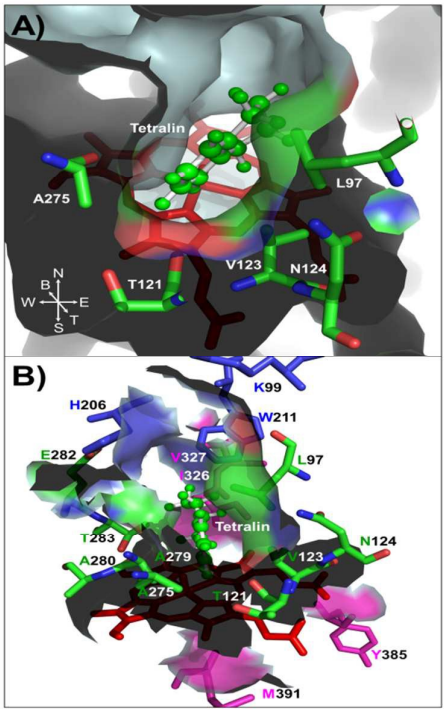

Fig. 1 Selected amino acid residues in the active pocket of $P450_{LaMO}$ for protein engineering. A) Selected residues lining the active pocket were used for the Phe scan. B) Selected residues were subjected to saturation mutagenesis on either single site or double sites shown in different areas: surrounding the heme ring (pink), internal acive pocket (green), outside active pocket (blue).

To probe the catalytic mechanism of wildtype and mutants, the kinetic isotope effects (KIEs) was measured, giving KIE values of 3.1 and 2.8/2.7 for WT and (*S*)-/(*R*)-selective mutants, respectively (Fig. S2† and Table S7†).[25] It is suggested that these P450s with different stereopreference still share the same process of C-H bond breaking.

Table 1 Catalytic performance of wildtype and mutants evolved for asymmetric hydroxylation of substrate **1a**

Entry	$P450_{LaMO}$	TOF (min^{-1})[a]	TTN[b]	*er*[c]
1	WT	0.04	116	66:34
2	RJ1	0.23	724	93:7
3	RJ2	0.17	852	95:5
4	RJ3	0.71	1360	98:2
5	RJ33	0.84	2104	95:5

[a] TOF: turnover frequency, measured within 5 min. [b] TTN, total turnover number was calculated after 24 h. More details see the Experimental Section. [c] Enantioselectivity was analyzed by HPLC, with an OD-H column, ESI. (*S*)-tetralol was formed for all entries.

During the characterization of variants, we found that pH 7.4 of the working solution and ethanol as a cosolvent (<5%, v/v) increased the enantioselectivity and product selectivity, respectively (Fig. S5† and Fig. S6†). It was shown that the environmental conditions of P450s may affect the dynamic conformation of holoenzyme, leading to the changes in selectivity. Moreover, the *E. coli* cells harboring an empty plasmid could not transform the tetralol into tetralone which excluded another factor affecting the product selectivity (Fig. S7†).

Some of the $P450_{LaMO}$ mutants engineered for hydroxylation of **1a** were characterized by measuring the turnover frequency (Table 1). The mutant RJ3 improved the TOF from 0.04 min^{-1} (WT) to 0.71 min^{-1}, which represents about 18-fold improvement. The TTN was enhanced from 116 to 1360, which corresponds to a 12-fold improvement. For the mutant RJ33, compared with the wildtype, about 18-fold improvement on TTN (from 116 to 2104) and 21-fold enhancement on TOF (from 0.04 min^{-1} to 0.84 min^{-1}) were achieved, respectively. These results show that this strategy is effective for improving not only the enantioselectivity but also the catalytic activity. Moreover, all the mutants maintained the absolute regioselectivity toward 1-position, without forming any other product except the ketone (Fig. S3† and Table S4†).

To explore the substrate profile, the best mutant RJ33 was employed to transform several other alkylbenzene compounds (**1b**-**1e**). The measured enantioselectivity and product selectivity are presented in Table 2. It shows that moderate to high degrees of enantioselectivity and product selectivity were achieved. In addition, the transformation of these substrates by $P450_{LaMO}$ gave better enantioselective (*S*)-product.

In order to provide insights into the (*S*)-enantioselective hydroxylation of $P450_{LaMO}$, we performed *in silico* modelling of the monooxygenase, and docked substrate **1a** into the modelled structures of wildtype and mutant RJ3 (Fig. 2). In the substrate binding poses of wildtype and RJ3 (T121V/Y385F/M391L), the average distances between the substrate C-H bond and the center of heme were 4.20 Å (average 4.7 Å and 3.7 Å) and 3.95 Å, respectively (Fig. 2A and Fig. 2B). Moreover, mutation T121V gave a hydrophobic residue Val121 which improves the hydrophobic effect in the active pocket. It cooperates with other two residues F385 and L391 around heme to provide a hydrophobic environment which is more liable for conducting hydroxylation of non-polar substrates. To get the clues for improvements of the enantioselectivity, (*S*)-tetralol was docked into the modelled structures of wildtype and mutants, respectively. The hydroxyl group was formed on the position of C-H bonds by both wildtype and mutant RJ3 (Fig. 2C and Fig. 2D). The mutant RJ3 shows a shorter distance between *O*- atom of (*S*)-hydroxy and the center of heme after reshaping the active pocket (from 3.6 to 2.6 Å), as compared to that of the wildtype (3.7 to 2.9 Å). Moreover, the hydrophobic effects promote the entering of substrate into the active pocket in a more appropriate manner to perform the H abstraction from C-H bonds. These results show that the mutant RJ3 is more favorable for forming the (*S*)-tetralol product.

View Article Online
DOI: 10.1039/C8CY01448E

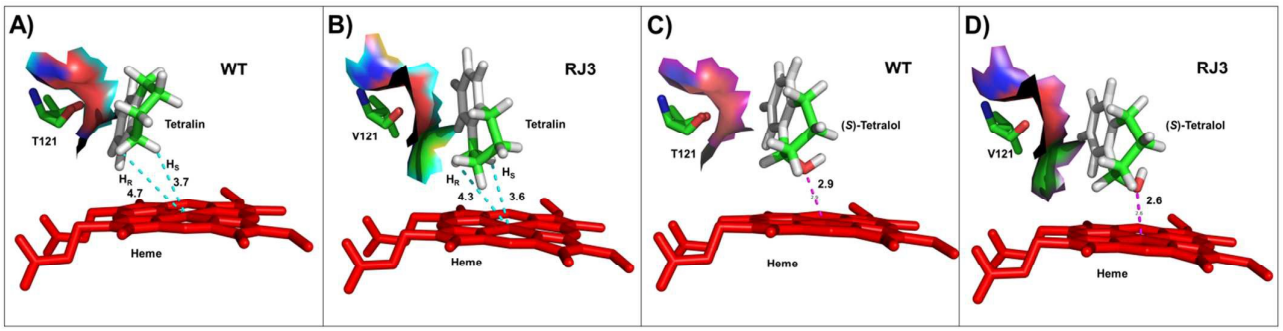

Fig. 2 Molecular docking poses of wildtype and mutant of $P450_{LaMO}$. (A) Molecular docking pose of wildtype for substrate **1a**. (B) Molecular docking pose of mutant RJ3 for substrate **1a**. C) Molecular docking pose of wildtype for (*S*)-**2a**. D) Molecular docking pose of mutant RJ3 docking pose for (*S*)-**2a**. All the results were based on *in silico* mutation of a homology model.

Table 2 Catalytic parameters of variant RJ33 for substrates **1b**–**1e**

Substrate	Structure	$P450_{LaMO}$	Product	*er* (*S*:*R*)[11a,26]	*ak* [c]	TTN [d]
1b		WT		56:44 [a]	67:33	333
		RJ33		92:8 [a]	83:17	999
1c		WT		86:14 [b]	75:25	133
		RJ33		93:7 [b]	87:13	399
1d		WT		87:13 [b]	92:8	1867
		RJ33		96:4 [b]	99:1	5533
1e		WT		94:6 [b]	100	267
		RJ33		96:4 [b]	100	333
		WT		75:25 [b]	93:7	1067
		RJ33		91:9 [b]	95:5	1000

[a] *er*: enantiometric ratio, analysed by HPLC with OD-H column. [b] Enantioselectivity measured by GC with chiral CP column. [c] *ak* value: the molar ratio of alcohol over ketone (defined as product selectivity), analysed by GC with Rsi-MS column. [d] TTN, calculated after 24 h. The reaction mixture (1 mL) was composed of 2 mM substrate, 0.5 mM $NADP^+$, 20 mM glucose, 15 U GDH, 0.3 µM P450s (cell free extracts), and 100 mM potassium phosphate buffer, pH 8.0.

Conclusions

In summary, because of the potential applications of (*S*)-tetralol as biologically active compounds, the biocatalytic hydroxylation of 1,2,3,4-tetrahydronaphthalene (**1a**) was attempted utilizing $P450_{LaMO}$ as a catalyst with oxygen as oxidant. Since the wildtype enzyme yielded only poor enantioselectivity (*er* 66:34) in favor of (*S*)-**2a** and moderate product selectivity (*ak* 76:24), protein engineering was performed through reshaping the active pocket to generate $P450_{LaMO}$ mutants with increased (*S*)-selectivity (up to *er* 98:2) as well as mutants showing reversed (*R*)-selectivity (*er* 23:77). Meanwhile, the *ak* value was enhanced up to 99:1 through the introduction of key residues (Fig. S2†). To probe the catalytic mechanism of wildtype and mutants, the kinetic isotope effect (KIE) was measured, giving KIE values of 3.1 and 2.8/2.7 for WT and (*S*)-/(*R*)-selective mutants, respectively (Fig. S3†, Table S4†).[25] It is suggested that these P450s with different stereopreference still share the same process of C-H bond breaking. For alkylbenzene-like C-H substrates (**1b**, **1c**, **1d**, **1e**), the mutants also enhanced the product selectivity and enantioselectivity. The resulting mutants are therefore an alternative to the chemical catalysts for performing C-H bond activation.[27] Furthermore, the Phe-based mutation strategy as described in this work may be beneficial for applications in future directed evolution of other potential industrial important enzymes.

View Article Online
DOI: 10.1039/C8CY01448E

Conflicts of interest

There are no conflicts to declare.

Acknowledgements

This work was financially supported by the National Natural Science Foundation of China (Nos. 21672063 & 21536004), the Fundamental Research Fund for the Central Universities (No. 222201514039), and the Science and Technology Commission of Shanghai Municipality (No. 15JC1400403). We thank Taiwo Dele-Osibanjo (Tianjin Institute of Industrial Biotechnology) for discussing the manuscript.

References

1 (a) P. F. Mugford, U. G. Wagner, Y. Jiang, K. Faber, R. J. Kazlauskas, *Angew. Chem. Int. Ed.*, 2008, **47**, 8782–8793; (b) K. Faber, W. Kroutil, *Curr. Opin. Chem. Biol.*, 2005, **9**, 181–187; (c) S. Panke, M. Held, M. Wubbolts, *Curr. Opin. Biotechnol.*, 2004, **15**, 272–279; (d) R. Weiss, S. Panke, *Curr. Opin. Biotechnol.*, 2009, **20**, 447–448; (e) M. Hönig, P. Sondermann, N. J. Turner, E. M. Carreira, *Angew. Chem. Int. Ed.*, 2017, **56**, 8942–8973; (f) P. Wei, Y. H. Cui, M. H. Zong, P. Xu, J. Zhou, W. Y. Lou, *Bioresour. Bioprocess.*, 2017, **4**, 39.

2 (a) S. M. Hosseini, H. H. Monfared, V. Abbasi, M. R. Khoshroo, Inorg. *Chem. Commun.*, 2016, **67**, 72–79; (b) Q. T. He, X. P. Li, L. F. Chen, L. Zhang, W. Wang, C. Y. Su, *ACS Catal.*, 2013, **3**, 1–9; (c) S. D. Munday, S. Dezvarei, S. G. Bell, *ChemCatChem*, 2016, **8**, 2789-2796.

3 (a) R. Fasan, *ACS Catal.*, 2012, **2**, 647–666; (b) G. D. Roiban, M. T. Reetz, *Chem. Commun.*, 2015, **51**, 2208–2224; (c) C. J. Whitehouse, S. G. Bell, L. L. Wong, *Chem. Soc. Rev.*, 2012, **41**, 1218–1260.

4 (a) M. W. Peters, P. Meinhold, A. Glieder, F. H. Arnold, *J. Am. Chem. Soc.*, 2003, **125**, 13442–13450; (b) R. Fasan, M. M. Chen, N. C. Crook, F. H. Arnold, *Angew. Chem. Int. Ed.*, 2007, **46**, 8414–8418; (c) R. E. White, J. P. Miller, L. V. Favreau, A. Bhattacharyya, *J. Am. Chem. Soc.*, 1986, **108**, 6024–6031; (d) Y. Liu, Y. C. Liu, Z. L. Wu, *Bioresour. Bioprocess.*, 2016, **3**, 10.

5 M. P. Mayhew, A. E. Roiberg, Y. Tewari, M. J. Holden, D. J. Vanderah, V. L. Vilker, *New J. Chem.*, 2002, **26**, 35–42.

6 (a) Y. Yang, J. Liu, Z. Li, *Angew. Chem. Int. Ed.*, 2014, **53**, 3120–3124; (b) Y. Yang, Y. T. Chi, H. H. Toh, Z. Li, *Chem. Commun.*, 2015, **51**, 914–917.

7 (a) G. Doru Roiban, R. Agudo, A. Ilie, R. Lonsdale, M. T. Reetz, *Chem. Commun.*, 2014, **50**, 14310–14313; (b) Y. Li, B. Qin, X. Li, J. Tang, Y. Chen, L. Zhou, S. You, *ChemCatChem*, 2018, **10**, 559–565.

8 (a) J. L. Vermilion, D. P. Ballou, V. Massey, M. J. Coon, *J. Biol. Chem.*, 1981, **256**, 266–277; (b) G. P. Kurzban, H. W. Strobel, *J. Biol. Chem.*, 1986, **261**, 7824–7830; (c) M. L. Klein, A. J. Fulco, *J. Biol. Chem.*, 1993, **268**, 7553–7561; (d) T. W. B. Ost, J. Clark, C. G. Mowat, C. S. Miles, M. D. Walkinshaw, G. A. Reid, S. K. Chapman, S. Daff, *J. Am. Chem. Soc.*, 2003, **125**, 15010–15020.

9 P. S. Coelho, E. M. Brustad, A. Kannan, F. H. Arnold, *Science*, 2013, **339**, 307–310.

10 Z. Sun, R. Lonsdale, G. Li, X. D. Kong, J. H. Xu, J. Zhou and M. T. Reetz, *Angew. Chem. Int. Ed.*, 2015, **54**, 12410–12415.

11 (a) Y. C. Yin, H. L. Yu, Z.J. Luan, R. J. Li, P. F. Ouyang, J. Liu, J. H. Xu, *ChemBioChem*, 2014, **15**, 2443-2449; (b) S. C. Hammer, G. Kubik, E. Watkins, S. Huang, H. Minges, F. H. Arnold, *Science*, 2017, **358**, 215–218.

12 (a) G. A. Roberts, A. Celik, D. J. B. Hunter, T. W. B. Ost, J. H. White, S. K. Chapman, N. J. Turner, S. L. Flitsch, *J. Biol. Chem.*, 2003, **278**, 48914–48920; (b) A. J. Warman, J. W. Robinson , D. Luciakova, A. D. Lawrence, K. R. Marshall, M. J. Warren, M. R. Cheesman, S. E. J. Rigby, A. W. Munro, K. J. McLean, *FEBS J.*, 2012, **279**, 1675–1693; (c) L. Liu, R. D. Schmid, V. B. Urlacher, *Appl. Microbiol. Biotechnol.*, 2006, **72**, 876–882; (d) D. Minerdi, S. J. Sadeghi, G. D. Nardo, F. Rua, S. Castrignano, P. Allegra, G. Gilardi, *Mol. Microbiol.*, 2015, **95**, 539–554.

13 J. M. Klenk, B. A. Nebel, J. L. Porter, J. K. Kulig, S. A. Hussain, S. M. Richter, M. Tavanti, N. J. Turner, M. A. Hayes, B. Hauer, S. L. Flitsch. *Biotechnol. J.*, 2017, **12**, 1600520.

14 a) A. Celik, G. A. Roberts, J. H. White, S. K. Chpman, N. J. Turner, S. L. Flitsch, *Chem. Commun.*, 2006, **43**, 4492–4494; (b) R. J. Li, J. H. Xu, Y. C. Yin, N. Wirth, J. M. Ren, B. B. Zeng, H. L. Yu, *New J. Chem.*, 2016, **40**, 8928–8934.

15 (a) A. T. Li, J. D. Zhang, J. H. Xu, W. Y. Lu, G. Q. Lin, *Appl. Environ. Microbiol.*, 2009, **75**, 551–556; (b) J. D. Zhang, A. T. Li, Y. Yang, J. H. Xu, *Appl. Microbiol. Biotechnol.*, 2010, **85**, 615–624; (c) J. D. Zhang, A. T. Li, J. H. Xu, *Bioprocess Biosyst. Eng.*, 2010, **33**, 1043–1049.

16 (a) D. G. Barrett, J. G. Catalano, D. N. Deaton, S. T. Long, R. B. McFadyen, A. B. Miller, L. R. Miller, K. J. WellsKnecht, L. L. Wright, *Bioorg. Med. Chem. Lett.*, 2005, **15**, 2209–2213; (b) Tibotec Pharmaceuticals Ltd, WO2008/99019 A1, 2008; (c) T. Naoki, J. Yao, US 2011/0178090 A1, 2011.

17 (a) G. D. Roiban, R. Agudo, A. Ilie, R. Lonsdale, M. T. Reetz, *Chem. Commun.*, 2014, **50**, 14310–14313; (b) W. Zhang, W. L. Tang, D. I. C. Wang, Z. Li, *Chem. Commun.*, 2011, **47**, 3284–3286; (c) F. Lie, Y. Chen, Z. Wang, Z. Li, *Tetrahedron: Asymmetry*, 2009, **20**, 1206–1211; (d) C. M. Noguera, M. M. Ferrari, M. K. Sanz, A. A. Orden, *J. Biotechnol.*, 2012, **160**, 189–194.

18 (a) M. T. Reetz, Directed Evolution of Selective Enzymes: Catalysts for Synthetic Organic Chemistry and Biotechnology, Wiley-VCH, Weinheim, 2016; (b) E. M. Brustad, F. H. Arnold, *Curr. Opin. Chem. Biol.*, 2011, **15**, 201–210; (c) A. S. Bommarius, Annu. *Rev. Chem. Biomol. Eng.*, 2015, **6**, 319–345; (d) E. M. J. Gillam, J. N. Copp, D. F. Ackerley, Methods of Molecular Biology, Humana Press, Totowa, 2014; (e) A. Currin, N. Swainston, P. J. Day, D. B. Kell, *Chem. Soc. Rev.*, 2015, **44**, 1172–1239; (f) N. J. Turner, *Nat. Chem. Biol.*, 2009, **5**, 567–573; (g) C. A. Denard, H. Ren, H. Zhao, *Curr. Opin. Chem. Biol.*, 2015, **25**, 55–64; (h) S. Lutz, U. T. Bornscheuer, Protein Engineering Handbook, Wiley-VCH, Weinheim, 2009;

View Article Online
DOI: 10.1039/C8CY01448E

(i) J. Wang, A. Ilie, M. T. Reetz, *Adv. Synth. Catal*., 2017, **359**, 2056–2060; (j) Z. Sun, P. T. Salas, E. Siirola, R. Lonsdale, M. T. Reetz, *Bioresour. Bioprocess.*, 2016, **3**, 44.

19 (a) Z. Sun, R. Lonsdale, G. Li, X. D. Kong, J. H. Xu, J. Zhou, M. T. Reetz, *Angew. Chem. Int. Ed.*, 2015, **54**, 12410–12415; (b) Z. Sun, R. Lonsdale, G. Li, M. T. Reetz, *ChemBioChem*, 2016, **17**, 1865–1872; (c) Z. Sun, R. Lonsdale, L. Wu, G. Li, A. Li, J. Wang, J. Zhou, M. T. Reetz, *ACS Catal.*, 2016, **6**, 1590–1597; (d) Z. Sun, R. Lonsdale, A. Ile, G. Li, J. Zhou, M. T. Reetz, *ACS Catal.*, 2016, **6**, 1598–1605; (e) G. Qu, R. Lonsdale, P. Yao, G. Li, B. Liu, M. T. Reetz, Z. Sun, *ChenBioChem*, 2018, **19**, 239–246; (f) A. Li, A. Ile, Z. Sun, R. Lonsdale, J. H. Xu, M. T. Reetz, *Angew. Chem. Int. Ed*., 2016, **55**, 1–5.

20 H. Y. Liu, A. Rashidbaigi, *Biotechniques,* 1990, **8**, 24–25

21 P. Guengerich, M. V. Martin, C. D. Sohl, Q. Cheng, *Nat. Protoc.*, 2009, **4**, 1245–1251

22 R. J. Li, J. H. Xu, Q. Chen, J. Zhao, A. Li, H. L. Yu, *ChemCatChem,* 2018, **10**, 2962–2968.

23 Z. Sun, R. Lonsdale, G. Li, M. T. Reetz, *ChemBioChem*, 2016, **17**, 1865–1872.

24 M. T. Reetz, *Angew. Chem. Int. Ed.*, 2011, **50**, 138–174.

25 (a) X. Huang, J. T. Groves, *Chem. Rev.*, 2017, **118**, 2491–2553; (b) K. H. Kim, E. M. Isin, C. H. Yun, D. H. Kim, F. P. Guengerich. *FEBS J.*, 2006, **273**, 2223–2231; (c) F. P. Guengerich, *J. Label Compd. Radiopharm*, 2013, **56**, 428–431; (d) R. Esala, P. Chandrasena, K. P. Vatsis, M. J. Coon, P. F. Hollenberg, M. Newcomb, *J. Am. Chem. Soc.*, 2004, **126**, 115–126; (e) Q. T. He, X. P. Li, L. F. Chen, L. Zhang, W. Wang, C. Y. Su, *ACS Catal.*, 2013, **3**, 1–9; (f) A. D. N. Vaz, M. J. Coon, *Biochemistry*, 1994, **33**, 6442–6449; (g) B. Meunier, S. P. D. Visser, S. Shaik, *Chem. Rev.*, 2004, **104**, 3947–3980.

26 J. Y. Liu, G. W. Zheng, C. X. Li, H. L. Yu, J. Pan, J. H. Xu, *J. Mol. Catal B: Enzymatic*, 2013, **89**, 41–47 .

27 (a) Ö. Dilek, M. A. Tezeren, T. Tilki, E. Ertürk, *Tetrahedron*, 2018, **74**, 268–286; (b) W. Zhang, B. O. Burek, E. F. Fueyo, *Angew. Chem. Int. Ed.*, 2017, **56**, 15451–15455.

View Article Online
DOI: 10.1039/C8CY01448E

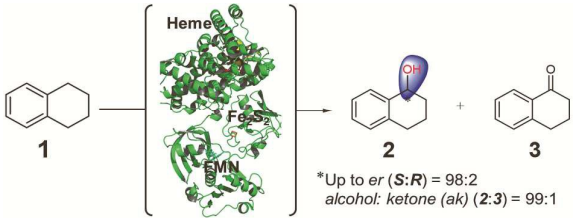

Via Phe scanning based protein engineering, P450$_{La}$MO increased the enantioselectivity to *er* 98:2, product selectivity, alcohol: ketone to *ak* 99:1.